

1 **Title: A Human Skin Model for Assessing the Arboviral Infections**

2 **Authors: Allen T. Esterly¹, Megan G. Lloyd¹ [ORCID ID: 0000-0002-6034-0846], Prashant Upadhyaya²**
3 **[ORCID ID: 0000-0002-6992-1196], Jennifer F. Moffat¹, Saravanan Thangamani^{1,3,4#}**

4 **Affiliations:**

5 ¹Department of Microbiology and Immunology,

6 ²Department of Surgery,

7 ³SUNY Center for Vector-Borne Diseases,

8 ⁴Institute for Global Health and Translational Medicine, SUNY Upstate Medical University, Syracuse, New

9 York, USA

10 #- Corresponding author: Saravanan Thangamani

11 *SUNY Upstate Medical University*

12 *505 Irving Ave, Syracuse NY 13210*

13 *Phone: 315-4647824*

14 *email: thangams@upstate.edu*

15

16

17

18

19

20 Key words: Mosquito feeding, skin, arbovirus, immunomodulation

21 Abbreviations used: Zika virus (ZIKV), Mayaro virus (MAYV), Chikungunya virus (CHIKV), Spondweni virus
22 (SPOV), Usutu virus (USUV), biological safety level 2 (BSL-2), Institutional Review Board (IRB), heat-
23 inactivated fetal bovine serum (HI-FBS), quantitative reverse transcriptase PCR (qRT-PCR), Leica
24 Application Suite X (LAS-X), multiplicity of infection (MOI), pattern recognition receptor (PRR),
25 Interferon-induced transmembrane proteins (IFITMs), standard error of the mean (SEM)

26

27 **Abstract:**

28 Arboviruses such as flaviviruses and alphaviruses cause a significant human healthcare burden
29 on the global scale. Transmission of these viruses occurs during human blood feeding at the mosquito-
30 skin interface. Not only do pathogen immune evasion strategies influence the initial infection and
31 replication of pathogens delivered, but arthropod salivary factors also influence transmission foci. In-
32 vitro cell cultures do not provide an adequate environment to study complex interactions between viral,
33 mosquito, and host factors. To address this need for a whole tissue system, we describe a proof-of-
34 concept model for arbovirus infection using adult human skin ex vivo with Zika virus (flavivirus) and
35 Mayaro virus (alphavirus). Replication of these viruses in human skin was observed up to 4 days post-
36 infection. Egressed viruses could be detected in the culture media as well. Antiviral and pro-
37 inflammatory genes, including chemoattractant chemokines, were expressed in infected tissue.
38 Immunohistochemical analysis showed the presence of virus in the skin tissue at 4 days post-infection.
39 This model will be useful to further investigate: 1) the immediate molecular mechanisms of arbovirus
40 infection in human skin, and 2) the influence of arthropod salivary molecules during initial infection of
41 arboviruses in a more physiologically relevant system.

42 **Introduction**

43 Arboviruses inflict a substantial global health burden on the human population. The re-emergence
44 of Zika virus (ZIKV) in 2014-2015 in Brazil is evidence that previously identified pathogens can re-emerge
45 to become significant health burdens on susceptible populations (Weaver et al., 2016). Other
46 arboviruses, such as Usutu virus (USUV), Spondweni virus (SPOV), and Mayaro virus (MAYV), continue to
47 emerge (Pierson & Diamond, 2020). MAYV is a New World arthritogenic alphavirus with current
48 autochthonous cycles of transmission in Central and South America (Diagne et al., 2020). Research on
49 emerging arboviruses is needed to better understand transmission cycles that threaten human health.

50 Mosquitoes inject saliva made up of a complex mixture containing pathogens, bioactive proteins,
51 and small RNAs to facilitate blood-feeding and pathogen transmission (Arcà & Ribeiro, 2018; Maharaj et
52 al., 2015). These bioactive molecules regulate hemostasis and modulate mammalian immune responses
53 at the mosquito-host-pathogen interface (Huang et al., 2019; Pinggen et al., 2017). The transmission
54 interface has been investigated using in-vitro tissue culture or animal infection models, but these
55 systems do not fully represent the human skin tissue environment. Therefore, this study intends to
56 model arbovirus infection in human skin ex vivo to investigate the immediate immunological events
57 during transmission.

58 Since the majority of mosquito-borne arboviruses transmitted to humans are from the genus
59 Flavivirus or Alphavirus, we used an established flavivirus of medical relevance (ZIKV) and an emerging
60 alphavirus (MAYV). MAYV and ZIKV infect human skin and replicate up to 4 days post-infection, shedding
61 from the skin to culture media. Chemoattractant chemokines, along with pro-inflammatory and antiviral
62 genes, were expressed in both MAYV and ZIKV infected skin as expected. In addition,
63 immunohistochemical analysis revealed staining positive for the virus in skin 4 days post-infection in
64 both virus-infected groups. This model will be further utilized to determine how mosquito salivary
65 factors influence viral replication kinetics or pro-inflammatory and chemoattractant molecule
66 expression during infection.

67 **Materials & Methods**

68 *Ethics Statement*

69 All experiments involving de-identified human specimens were conducted in a biological safety
70 level 2 (BSL-2) laboratory in accordance with a protocol approved by the SUNY Upstate Medical
71 University Institutional Review Board (IRB).

72 *Culturing of Cells and Viruses*

73 Vero, Vero E6, and C6/36 cells were obtained from ATCC and passaged in DMEM with 10% heat-
74 inactivated fetal bovine serum (HI-FBS) and 1% penicillin-streptomycin at 37°C + 5% CO₂ (Vero & Vero
75 E6) or in Leibovitz L-15 media with 10% HI-FBS and 1% penicillin-streptomycin at 28°C (C6/36)
76 (Ammerman et al., 2008). Zika virus (Mex I44) was obtained from the World Reference Center for
77 Emerging Viruses and Arboviruses at the University of Texas Medical Branch in Galveston, Texas. Mayaro
78 virus (Uruma) was obtained from the Centers for Disease Control, Fort Collins, Colorado. Viruses were
79 cultured in Vero cells (ATCC CCL-81) for 4 passages and then passaged once in C3/36 cells as referenced
80 (Coelho et al., 2017; Svenson et al., 2018). In addition, virus titers were obtained via focus-forming assay
81 in Vero E6 cells as previously described (Rossi et al., 2012).

82 *Preparation and Infection of human skin*

83 De-identified adult human skin was donated by fully informed patients undergoing reduction
84 mammoplasty at the Upstate Medical University Hospital (Syracuse, NY). All skin specimens were
85 collected within approximately 2 h post-surgery. Underlying adipose was grossly dissected, and each
86 specimen was washed in PBS and incubated in skin culture media (RPMI 1640 media containing 10% HI-
87 FBS, 1% penicillin-streptomycin, and 0.25µg/mL of Amphotericin B)(Lloyd et al., 2020). The epidermis
88 and upper dermal layers were removed using a skin grafting knife, cut into 1-cm² biological samples,
89 then placed in Netwells® (Corning, 15-mm x 500 µm mesh size) suspending the skin at a liquid-air
90 interface. Netwells were placed in 12-well tissue culture plates containing 1 mL skin culture media. The
91 skin was cultured ex vivo for 4 days in skin culture media at 33°C with 5% CO₂ as previously described
92 (Lloyd et al., 2020). Next, the skin was infected intradermally using a 28-gauge insulin syringe with 25 µL
93 (±2 µL) of uninfected skin culture media (mock), ZIKV, or MAYV adjusted to deliver 10³ FFU. Skin samples
94 were processed as outlined below at 2- and 4-days post-infection. Each experimental group contained
95 multiple biological replicates (n=4) and independent infections were repeated using skin specimens from
96 3 donors.

97 *RNA Isolation, qRT-PCR, and Gene Expression Analysis*

98 At days 2 and 4 post-infection, skin samples were cut in half using a scalpel and placed in either
99 10% neutral buffered formalin or OCT media for histological analysis or in TRIzol reagent for RNA
100 isolation. RNA was extracted from the skin and skin culture media samples using TRIzol and TRIzol LS
101 reagents, respectively, combined with Qiagen RNeasy mini kits to inactivate the virus and obtain high
102 yields of RNA(Heinze et al., 2012; Hermance et al., 2020). RNA purity and concentration were verified on
103 a Denovix DS-11+ spectrophotometer.

104 Absolute quantification of viral loads was performed using quantitative reverse transcriptase
105 PCR (qRT-PCR) using a BioRad CFX96. Viral genomes were amplified with the BioRad One-Step Universal
106 Probes kit using primers: ZIKV 1086, ZIKV 1162c, and probe ZIKV 1107-FAM or MAYV Forward (5'-
107 AAGCTCTTCTCTGCATTGC-3', MAYV Reverse 2 (5'-TGCTGGAAATGCTCTTTGTA-3'), and MAYV Probe (5'-
108 GCCGAGAGCCCGTTTTTAAAATCAC-3') previously established (Lanciotti et al., 2008; Waggoner et al.,
109 2018). The MAYV primer-probe combination was slightly modified to utilize a Cy5/Iowa Black RQ
110 fluorophore/quencher combination from Integrated DNA Technologies (Coralville, Iowa). RNA isolated
111 from an aliquot of both ZIKV and MAYV, from the exact passage used for infection, was serially diluted,
112 and used to design a standard curve to quantify viral loads in tissue and supernatant.

113 cDNA conversion of tissue RNA was performed according to the manufacturer's specification
114 using the BioRad iScript cDNA synthesis kit using approximately 1µg of RNA. cDNA was diluted 5-fold,
115 and gene expression analysis was performed using BioRad iTaq Universal SYBR Green Supermix
116 according to the manufacturer's specifications. Briefly, 1 µg of RNA/sample was used for the reverse
117 transcriptase reaction. cDNA was diluted in RNase-free water at a 1:5 ratio, and a standard volume was
118 used for each downstream qPCR reaction. Primers used for gene expression analysis are

119 listed in Table 1. Expression was normalized using a eukaryotic ribosomal 18s as a ‘housekeeping’ gene
120 with data shown as a ratio of gene target fold change in infected tissue relative to mock-infected tissue
121 using the Livak ($2^{-\Delta\Delta Cq}$) method (Livak & Schmittgen, 2001).

122 *Histology and Immunohistochemistry*

123 Tissues fixed in formalin were paraffin-embedded and cut in 5 μ m thick sections to be placed on
124 glass slides (Hermance et al., 2016). Samples were deparaffinized and dehydrated in xylene and graded
125 ethanol washes. Hematoxylin and Eosin (H&E) staining was performed according to the manufacturer’s
126 specifications (Vector Laboratories H-3502). Immunohistochemical detection of ZIKV and MAYV was
127 performed using 5 μ m frozen sections of tissues snap-frozen in OCT media immediately after the
128 indicated endpoint. Briefly, tissue sections were fixed in methanol then washed in TBS+0.05% Tween20.
129 Wash buffer was applied between all blocking and antibody incubation steps. Sections were treated
130 with BLOXALL solution (Vector Labs, Burlingame, CA) to block endogenous peroxidases and alkaline
131 phosphatases. Primary and secondary antibodies (murine immune ascites fluid generated against ZIKV
132 or MAYV; goat anti-mouse HRP conjugate, respectively) were incubated for 1 h. Detection was
133 performed with Vector Labs ImmPACT AMEC Red substrate, peroxidase kit. Cover slides were mounted
134 using Vector Labs H5000 permanent mounting medium. Mock infected tissues were sectioned and
135 treated, in parallel, with the same antibody incubation and wash steps as listed above. All images were
136 taken using a Leica DM2500 LED/DMC5400 brightfield microscope and Leica Application Suite X (LAS-X)
137 software.

138 *Data Analysis*

139 Statistical significance of viral growth kinetics was performed using 2-way ANOVA with Šidák’s
140 multiple comparisons test in GraphPad Prism 9.1.2. Statistical significance of gene expression data was
141 analyzed by an F-test to determine variance, followed by a student’s t-test to assess the increase of the

142 target gene from 2-4-days post-infection. Welch's correction was applied when the F-test hypothesis
143 was failed to be rejected.

144 Data availability Statement: Data generated in study are paresend within this manuscript.
145

146 **Results and Discussion**

147 *Viability of human skin explant*

148 This study utilized human skin donated from elective breast reduction surgeries and cultured it ex
149 vivo as previously described (Lloyd et al., 2020). Human skin was viable when cultured ex vivo for at
150 least 4 days. Tissue sections stained with H&E showed minor histopathological changes after 4 days in
151 culture. In addition, some papillary dermal edema and minimal lymphocytic infiltrate in the superficial
152 dermis was observed; however, no major pathological changes, such as acanthosis or psoriasiform
153 hyperplasia, were apparent (Figure 1).

154 *MAYV and ZIKV replication in human skin*

155 To determine the susceptibility of human skin to arbovirus infection, skin pieces were intradermally
156 inoculated with 1000 FFU of MAYV or ZIKV, a physiologically relevant dose delivered from a mosquito
157 (Castanha et al., 2020; Styer et al., 2007). Viral RNA in the skin tissue was measured by qRT-PCR and
158 increased for both MAYV and ZIKV during the 4-day incubation period (Figure 2). We also found that
159 viral RNA in the skin culture media increased for both infections (Figure 2). Furthermore, in cryo-
160 sectioned skin, immunohistochemical detection of MAYV and ZIKV showed widespread infected cells
161 after 4 days (Figure 3), consistent with viral RNA detection in the homogenized tissue (Figure 2).
162 Therefore, cultured human skin was viable and susceptible to arbovirus infection for up to 4 days.

163 Human skin processed similarly and infected with DENV-2 showed the presence of negative-strand
164 RNA at 48h and 72h post-infection, indicative of viral replication (Limon-Flores et al., 2005). ZIKV infects

165 several skin cell populations. Infection in primary cultures of epidermal keratinocytes and dermal
166 fibroblasts show increasing viral RNA loads and infectious titer over time (Hamel et al., 2015). Dermal
167 dendritic and Langerhans cells, present in the dermis and epidermis, respectively (Pasparakis et al.,
168 2014), are also permissive to ZIKV infection when derived from PBMCs (Hamel et al., 2015). Our results
169 showed increased replication of ZIKV in human skin explants over time which parallel previous findings
170 (Hamel et al., 2015), but also suggests these viruses spread from the inoculation site and egress into the
171 media. MAYV infection in human skin is not well characterized and to our knowledge, our data is the
172 first to show MAYV infection in human skin *ex vivo*. Alphaviruses such as CHIKV also replicate in human
173 skin cell populations (Matusali et al., 2019). Human skin fibroblasts, both primary and immortal, are
174 susceptible to CHIKV *in vitro* (Ekchariyawat et al., 2015; Sourisseau et al., 2007; Wichit et al., 2017).
175 CHIKV-infected human skin explants showed the presence of viral RNA at 24h and 48h post-infection
176 when infected with a larger inoculum (10^5) (Bryden et al., 2020). Interestingly, both primary human and
177 immortalized keratinocytes poorly replicate CHIKV by restricting replication at a post-endosomal fusion
178 step despite the high multiplicity of infection *in vitro* (MOI=50)(Bernard et al., 2015).

179 *MAYV and ZIKV induce inflammatory expression in the skin*

180 Expression of pro-inflammatory signals from skin resident cell populations are critical for
181 recruiting circulating myeloid cells to the site of infection(Pasparakis et al., 2014). Since this model
182 utilizes skin detached from the microvasculature, one of the primary limitations is the influx of
183 inflammatory cells to the site of infection. Therefore, we assessed the expression of inflammatory
184 targets which recruit myeloid cell populations to the site of infection. Chemo-attractive chemokines
185 CCL2, CCL3, CCL4, and CXCL8 were upregulated during MAYV and ZIKV infection (Figure 4). In other
186 studies, DENV-infected keratinocytes express CCL2, CCL3, CCL4, CCL5, CXCL8 in a similar trend at 48h
187 post-infection (Duangkhae et al., 2018). The same DENV-infected culture also shows the expression of
188 IL-1 α , IL-1 β , IL-10, and CCL20 at the same timepoint (Duangkhae et al., 2018). WNV infection induces the

189 expression of antiviral cytokines such as IFN- β , IL-28a, and IL-29 at 24h and 48h post-infection in primary
190 keratinocytes (Garcia et al., 2018). Additionally, expression of CXCL1, CXCL2, CXCL8, and CCL20 and
191 cytokines IL-6 and TNF α are also induced at the same time points (Garcia et al., 2018).

192 Elevated expression levels of non-TLR receptors of viral ligands, RIG-I, MDA5, and PKR were also
193 found in ZIKV and MAYV infected tissues. RIG-I and MDA5 are cytosolic helicases that detect viral RNA
194 and are critical for triggering innate immune responses to flaviviruses and alphaviruses (Akhrymuk et al.,
195 2016; Chow et al., 2018; Kell & Gale, 2015). PKR is a pattern recognition receptor (PRR) and an IFN-
196 inducible-gene product that triggers signaling cascades responsible for further type I IFN activation and
197 inhibition of viral protein synthesis, among other functions (Munir & Berg, 2013). Both MAYV and ZIKV
198 infection induced an increase in the expression of RIG-I, MDA5, and PKR in these tissues (Figure 4). This
199 corresponds to previous findings of synthetic dsRNA poly(I:C) initiating antiviral signaling in
200 keratinocytes (Kalali et al., 2008). The natural expression of pro-inflammatory and antiviral genes in skin
201 explants provides a suitable model for studying human skin's immediate immune signaling events.

202 Interferon-induced transmembrane proteins (IFITMs) are strongly upregulated by type I and type II
203 interferon and localize to plasma and endocytic membranes to restrict virus entry (Bailey et al., 2014;
204 Zhao et al., 2019). Given IFITM molecules show restriction of ZIKV (Savidis et al., 2016) and MAYV (Franz
205 et al., 2021) infection, we assessed the expression of IFITM1, -2, and -3 in human skin tissue infected
206 with either ZIKV or MAYV (Figure 4). IFITM1 levels were elevated during ZIKV infection as expected,
207 however there was not a significant increase from 2 to 4 dpi. IFITM2 slightly increased above baseline at
208 4d post-infection, while IFITM3 remained near basal expression levels. MAYV infection induced a more
209 robust IFITM expression. IFITM1 was elevated at 2 and 4 dpi with statistically higher expression at 4 dpi.
210 IFITM2 and IFITM3 were slightly elevated at 2 dpi but significantly increased at 4 dpi. Further
211 experimentation would be necessary to better understand the role of these antiviral molecules in the
212 skin in relation to virus infection at the mosquito bite site.

213 **Conclusion**

214 Skin is the largest organ of the human body that interfaces with external stimuli, including pathogens,
215 and is permissive to arbovirus infection (Garcia et al., 2017). Blood-feeding mosquitoes deliver virus
216 from infected salivary glands along with a cocktail of pharmacologically active molecules. Several studies
217 show mosquito-derived salivary factors inducing greater morbidity and higher viremia when delivered
218 with a pathogen in animal models (Pingen et al., 2016). This highlights the importance of understanding
219 mosquito-specific factors active during transmission and the need to characterize such molecules in
220 human skin. Human skin can be used as an *ex vivo* experimental site of infection for alpha- and
221 flaviviruses. Both MAYV and ZIKV replicate in human skin to 4 days post-infection and shed into the skin
222 culture media. Infection in the skin leads to gene expression of chemotactic factors responsible for
223 recruiting inflammatory cells such as neutrophils and macrophages. In addition, innate antiviral
224 responses are active and induced after viral infection. Histological analysis showed no major
225 pathological changes; however, immunohistochemical analysis showed widespread MAYV and ZIKV
226 infection in human skin. Mosquito-borne virus replication in human skin can be utilized to further
227 investigate mosquito transmission to humans and the associated salivary mediators that work in concert
228 to facilitate blood acquisition and pathogen delivery.

229

230

231

232 **Figure Legends**

233 **Figure 1. Viability of human skin ex vivo.** Skin cultured *ex vivo* was harvested each day for up to 4 days.

234 Formalin fixed, paraffin-embedded tissue sections (5 μ m) were placed on glass slides for H&E staining.

235 Pathological interpretation was provided by a board-certified pathologist (HISTOWIZ, Brooklyn, NY).

236 Sections are representative of multiple biological samples from multiple skin specimens sectioned and
237 stained using the same methodology.

238

239 **Figure 2. Skin is susceptible to arboviruses.** Skin was infected intradermally with either MAYV (red) or
240 ZIKV (blue). Data points are mean values with error bars indicating standard deviations. Data represents
241 repeated independent experiments using n=4 biological replicates per group across multiple donated
242 tissues. A two-way ANOVA was used to determine statistical difference with Šidák's multiple
243 comparisons $**p < 0.001$.

244

245 **Figure 3. Expression of viral antigen in human skin.** Immunohistochemical detection of MAYV antigen
246 (middle column) and ZIKV antigen (right column) in cryo-sectioned skin post-infection. Arrows indicate
247 antigen detection at 10x and 40x magnification. Mock tissues were treated with either MAYV or ZIKV
248 antibodies in parallel to respective infected tissues. Skin sections are representative of multiple
249 biological replicates from independent experiments with consistent detection of viral antigen.

250

251 **Figure 4. qPCR inflammatory gene expression of arbovirus infected human skin.** qPCR analysis of MAYV
252 infected tissues (red) and ZIKV infected tissues (blue) at 2 and 4 days post-infection. Data shown is the
253 relative fold change (Livak method $2^{-\Delta\Delta Ct}$) of virus infected tissue compared to mock infected tissue,
254 normalized to 18s ribosomal RNA. Expression levels from 2d to 4d were compared for statistical
255 difference. Error bars indicate the standard error of the mean (SEM). Data is representative of
256 experimental means with standard deviations of independent experiments with repeat using n=4

257 biological replicates per group. Student's t test with Welch's correction was used to determine statistical
 258 difference *p<0.05; **p<0.001; ***p<0.0001.

259

260

261 **Table 1.** qPCR primers used for gene expression analysis.

Gene Target	Forward Primer (5'-3')	Reverse Primer (5'-3')	Reference
<i>CCL2</i>	GATCTCAGTGCAGAGGCTCG	TGCTTGCCAGGTGGTCCAT	(Dumoulin et al., 2000)
<i>CCL3</i>	CATCACTTGCTGCTGACACG	TGTGGAATCTGCCGGGAG	(Duangkhae et al., 2018)
<i>CCL4</i>	ACCCTCCCACCGCCTGCTGC	GTTGCAGGTCATACACGTA	(Dumoulin et al., 2000)
<i>CCL5</i>	ACCACACCCTGCTGCTTTGC	CCGAACCCATTCTTTGC	(Dumoulin et al., 2000)
<i>CCL20</i>	TTGGATCCTGCTGCTACTCCACCTCTG	TTCTCGAGTATATTTACCCAAGTCTGTTTT	(Akahoshi et al., 2003)
<i>CXCL8</i>	CTGGCCGTGGCTCTCTTGG	GGGTGGAAAGGTTTGGAGTATGTC	(Duangkhae et al., 2018)
<i>CXCL10</i>	GAAATTATCTCTGCAAGCCAATT	TCACCCTCTTTTTCATGTAGCA	(Clarke et al., 2010)
<i>Rig-I</i>	AGTGAGCATGCACGAATGAA	GGGATCCCTGGAAACACTTT	(Surasombatpattana et al., 2011)
<i>Mda5</i>	TGTATTCATTATGCTACAGAACTG	ACTGAGACTGGTACTTTGGATTCT	(Surasombatpattana et al., 2011)
<i>Ifn-β</i>	GACGCCGATTGACCATCTA	TTGGCCTTCAGGTAATGCAGAA	(Surasombatpattana et al., 2011)
<i>PKR</i>	TCTGACTACCTGTCCTCTGGTTCTT	GCGAGTGTGCTGGTCACTAAAG	(Surasombatpattana et al., 2011)
<i>Ifitm1</i>	GGGCATCCTCATGACCATTGGA	GGCTACTAGTAACCCCGTTTTCTCTG	(Prelli Bozzo et al., 2021)
<i>Ifitm2</i>	GTCACCATGAACCACATTGTGCAAAC	CCCCAGCATAGCCACTTCC	(Prelli Bozzo et al., 2021)
<i>Ifitm3</i>	ACCATGAATCACACTGTCCAAACCTT	CCAGCACAGCCACCTCG	(Prelli Bozzo et al., 2021)
<i>18s</i>	GGCCCGAAGCGTTTACTTTG	GCCGGTCCAAGAATTCACC	(Surasombatpattana et al., 2011)

262

263

264

265 References

- 266 Akahoshi, T., Sasahara, T., Namai, R., Matsui, T., Watabe, H., Kitasato, H., Inoue, M., & Kondo, H. (2003).
267 Production of Macrophage Inflammatory Protein 3 α (MIP-3 α) (CCL20) and MIP-3 β (CCL19) by
268 Human Peripheral Blood Neutrophils in Response to Microbial Pathogens. *Infection and Immunity*,
269 *71*(1), 524–526. <https://doi.org/10.1128/IAI.71.1.524-526.2003>
- 270 Akhrymuk, I., Frolov, I., & Frolova, E. I. (2016). Both RIG-I and MDA5 detect alphavirus replication in
271 concentration-dependent mode. *Virology*, *487*, 230–241.
272 <https://doi.org/10.1016/j.virol.2015.09.023>
- 273 Ammerman, N. C., Beier-Sexton, M., & Azad, A. F. (2008). Growth and Maintenance of Vero Cell Lines.
274 *Current Protocols in Microbiology*, *11*(1), 1–7. <https://doi.org/10.1002/9780471729259.mca04es11>
- 275 Arcà, B., & Ribeiro, J. M. (2018). Saliva of hematophagous insects: a multifaceted toolkit. In *Current*
276 *Opinion in Insect Science* (Vol. 29, pp. 102–109). <https://doi.org/10.1016/j.cois.2018.07.012>
- 277 Bailey, C. C., Zhong, G., Huang, I. C., & Farzan, M. (2014). IFITM-family proteins: The cell's first line of
278 antiviral defense. *Annual Review of Virology*, *1*(1), 261–283. <https://doi.org/10.1146/annurev-virology-031413-085537>
- 280 Bernard, E., Hamel, R., Neyret, A., Ekchariyawat, P., Molès, J. P., Simmons, G., Chazal, N., Desprès, P.,
281 Missé, D., & Briant, L. (2015). Human keratinocytes restrict chikungunya virus replication at a post-
282 fusion step. *Virology*, *476*, 1–10. <https://doi.org/10.1016/j.virol.2014.11.013>
- 283 Bryden, S. R., Pinggen, M., Lefteri, D. A., Miltenburg, J., Delang, L., Jacobs, S., Abdelnabi, R., Neyts, J.,
284 Pondeville, E., Major, J., Müller, M., Khalid, H., Tuplin, A., Varjak, M., Merits, A., Edgar, J., Graham,
285 G. J., Shams, K., & McKimmie, C. S. (2020). Pan-viral protection against arboviruses by activating
286 skin macrophages at the inoculation site. *Science Translational Medicine*, *12*(527).
287 <https://doi.org/10.1126/scitranslmed.aax2421>
- 288 Castanha, P. M. S., Erdos, G., Watkins, S. C., Falo, L. D., Marques, E. T. A., & Barratt-Boyes, S. M. (2020).
289 Reciprocal immune enhancement of dengue and Zika virus infection in human skin. *JCI Insight*,
290 *5*(3). <https://doi.org/10.1172/jci.insight.133653>
- 291 Chow, K. T., Gale, M., & Loo, Y. M. (2018). RIG-I and Other RNA Sensors in Antiviral Immunity. In *Annual*
292 *Review of Immunology* (Vol. 36, pp. 667–694). <https://doi.org/10.1146/annurev-immunol-042617-053309>
- 294 Clarke, D. L., Clifford, R. L., Jindarat, S., Proud, D., Pang, L., Belvisi, M., & Knox, A. J. (2010). TNF α and
295 IFN γ Synergistically Enhance Transcriptional Activation of CXCL10 in Human Airway Smooth Muscle
296 Cells via STAT-1, NF- κ B, and the Transcriptional Coactivator CREB-binding Protein. *Journal of*
297 *Biological Chemistry*, *285*(38), 29101–29110. <https://doi.org/10.1074/jbc.M109.099952>
- 298 Coelho, S. V. A., Neris, R. L. S., Papa, M. P., Schnellrath, L. C., Meuren, L. M., Tschoeke, D. A., Leomil, L.,
299 Verçoza, B. R. F., Miranda, M., Thompson, F. L., da Poian, A. T., Souza, T. M. L., Carneiro, F. A.,
300 Damaso, C. R., Assunção-Miranda, I., & de Arruda, L. B. (2017). Development of standard methods

- 301 for Zika virus propagation, titration, and purification. *Journal of Virological Methods*, 246(April),
302 65–74. <https://doi.org/10.1016/j.jviromet.2017.04.011>
- 303 Diagne, C. T., Bengue, M., Choumet, V., Hamel, R., Pompon, J., & Missé, D. (2020). Mayaro Virus
304 Pathogenesis and Transmission Mechanisms. *Pathogens*, 9(9), 738.
305 <https://doi.org/10.3390/pathogens9090738>
- 306 Duangkhae, P., Erdos, G., Ryman, K. D., Watkins, S. C., Faló, L. D., Marques, E. T. A., & Barratt-Boyes, S.
307 M. (2018). Interplay between Keratinocytes and Myeloid Cells Drives Dengue Virus Spread in
308 Human Skin. *Journal of Investigative Dermatology*, 138(3), 618–626.
309 <https://doi.org/10.1016/j.jid.2017.10.018>
- 310 Dumoulin, F. L., Nischalke, H. D., Leifeld, L., von dem Bussche, A., Rockstroh, J. K., Sauerbruch, T., &
311 Spengler, U. (2000). Semi-quantification of human C-C chemokine mRNAs with reverse
312 transcription/real-time PCR using multi-specific standards. *Journal of Immunological Methods*,
313 241(1–2), 109–119. [https://doi.org/10.1016/S0022-1759\(00\)00210-6](https://doi.org/10.1016/S0022-1759(00)00210-6)
- 314 Ekchariyawat, P., Hamel, R., Bernard, E., Wichit, S., Surasombatpattana, P., Talignani, L., Thomas, F.,
315 Choumet, V., Yssel, H., Desprès, P., Briant, L., & Missé, D. (2015). Inflammasome signaling pathways
316 exert antiviral effect against Chikungunya virus in human dermal fibroblasts. *Infection, Genetics
317 and Evolution*, 32, 401–408. <https://doi.org/10.1016/j.meegid.2015.03.025>
- 318 Franz, S., Pott, F., Zillinger, T., Schöler, C., Dapa, S., Fischer, C., Passos, V. ania, Stenzel, S., Chen, F.,
319 Döhner, K., Hartmann, G., Sodeik, B., Pessler, F., Simmons, G., Drexler, J. F., & Goffinet, C. (2021).
320 Human IFITM3 restricts chikungunya virus and Mayaro virus infection and is susceptible to virus-
321 mediated counteraction. *Life Science Alliance*, 4(7), 1–15. <https://doi.org/10.26508/lsa.202000909>
- 322 Garcia, M., Alout, H., Diop, F., Damour, A., Bengue, M., Weill, M., Missé, D., Lévêque, N., & Bodet, C.
323 (2018). Innate Immune Response of Primary Human Keratinocytes to West Nile Virus Infection and
324 Its Modulation by Mosquito Saliva. *Frontiers in Cellular and Infection Microbiology*, 8(November),
325 387. <https://doi.org/10.3389/fcimb.2018.00387>
- 326 Garcia, M., Wehbe, M., Lévêque, N., & Bodet, C. (2017). Skin innate immune response to flaviviral
327 infection. *European Cytokine Network*, 28(2), 41–51. <https://doi.org/10.1684/ecn.2017.0394>
- 328 Hamel, R., Dejarnac, O., Wichit, S., Ekchariyawat, P., Neyret, A., Luplertlop, N., Perera-Lecoin, M.,
329 Surasombatpattana, P., Talignani, L., Thomas, F., Cao-Lormeau, V.-M., Choumet, V., Briant, L.,
330 Desprès, P., Amara, A., Yssel, H., & Missé, D. (2015). Biology of Zika Virus Infection in Human Skin
331 Cells. *Journal of Virology*, 89(17), 8880–8896. <https://doi.org/10.1128/JVI.00354-15>
- 332 Heinze, D. M., Wikel, S. K., Thangamani, S., & Alarcon-chaidez, F. J. (2012). *Transcriptional profiling of
333 the murine cutaneous response during initial and subsequent infestations with Ixodes scapularis
334 nymphs*. 1–15. <https://doi.org/10.1186/1756-3305-5-26>
- 335 Hermance, M. E., Hart, C. E., Esterly, A. T., Reynolds, E. S., Bhaskar, J. R., & Thangamani, S. (2020).
336 Development of a small animal model for deer tick virus pathogenesis mimicking human clinical
337 outcome. *PLOS Neglected Tropical Diseases*, 14(6), e0008359.
338 <https://doi.org/10.1371/journal.pntd.0008359>

- 339 Hermance, M. E., Santos, R. I., Kelly, B. C., Valbuena, G., & Thangamani, S. (2016). Immune cell targets of
340 infection at the tick-skin interface during powassan virus transmission. *PLoS ONE*, *11*(5).
341 <https://doi.org/10.1371/journal.pone.0155889>
- 342 Huang, Y.-J. S., Higgs, S., & Vanlandingham, D. L. (2019). Arbovirus-Mosquito Vector-Host Interactions
343 and the Impact on Transmission and Disease Pathogenesis of Arboviruses. *Frontiers in*
344 *Microbiology*, *10*(January), 1–14. <https://doi.org/10.3389/fmicb.2019.00022>
- 345 Kalali, B. N., Köllisch, G., Mages, J., Müller, T., Bauer, S., Wagner, H., Ring, J., Lang, R., Mempel, M., &
346 Ollert, M. (2008). Double-Stranded RNA Induces an Antiviral Defense Status in Epidermal
347 Keratinocytes through TLR3-, PKR-, and MDA5/RIG-I-Mediated Differential Signaling. *The Journal of*
348 *Immunology*, *181*(4), 2694–2704. <https://doi.org/10.4049/jimmunol.181.4.2694>
- 349 Kell, A. M., & Gale, M. (2015). RIG-I in RNA virus recognition. *Virology*, *479–480*, 110–121.
350 <https://doi.org/10.1016/j.virol.2015.02.017>
- 351 Lanciotti, R. S., Kosoy, O. L., Laven, J. J., Velez, J. O., Lambert, A. J., Johnson, A. J., Stanfield, S. M., &
352 Duffy, M. R. (2008). Genetic and serologic properties of Zika virus associated with an epidemic, Yap
353 State, Micronesia, 2007. *Emerging Infectious Diseases*, *14*(8), 1232–1239.
354 <https://doi.org/10.3201/eid1408.080287>
- 355 Limon-Flores, A. Y., Perez-Tapia, M., Estrada-Garcia, I., Vaughan, G., Escobar-Gutierrez, A., Calderon-
356 Amador, J., Herrera-Rodriguez, S. E., Brizuela-Garcia, A., Heras-Chavarria, M., Flores-Langarica, A.,
357 Cedillo-Barron, L., & Flores-Romo, L. (2005). Dengue virus inoculation to human skin explants: An
358 effective approach to assess in situ the early infection and the effects on cutaneous dendritic cells.
359 *International Journal of Experimental Pathology*, *86*(5), 323–334. <https://doi.org/10.1111/j.0959-9673.2005.00445.x>
- 361 Livak, K. J., & Schmittgen, T. D. (2001). Analysis of relative gene expression data using real-time
362 quantitative PCR and the 2- $\Delta\Delta$ CT method. *Methods*, *25*(4), 402–408.
363 <https://doi.org/10.1006/meth.2001.1262>
- 364 Lloyd, M. G., Smith, N. A., Tighe, M., Travis, K. L., Liu, D., Upadhyaya, P. K., Kinchington, P. R., Chan, G. C.,
365 & Moffat, J. F. (2020). A novel human skin tissue model to study varicella zoster virus and human
366 cytomegalovirus. *Journal of Virology*, *September*. <https://doi.org/10.1128/JVI.01082-20>
- 367 Maharaj, P. D., Widen, S. G., Huang, J., Wood, T. G., & Thangamani, S. (2015). Discovery of Mosquito
368 Saliva MicroRNAs during CHIKV Infection. *PLoS Neglected Tropical Diseases*, *9*(1), 18–24.
369 <https://doi.org/10.1371/journal.pntd.0003386>
- 370 Matusali, G., Colavita, F., Bordi, L., Lalle, E., Ippolito, G., Capobianchi, M. R., & Castilletti, C. (2019).
371 Tropism of the chikungunya virus. *Viruses*, *11*(2). <https://doi.org/10.3390/v11020175>
- 372 Munir, M., & Berg, M. (2013). The multiple faces of protein kinase R in antiviral defense. *Virulence*, *4*(1),
373 85–89. <https://doi.org/10.4161/viru.23134>
- 374 Pasparakis, M., Haase, I., & Nestle, F. O. (2014). Mechanisms regulating skin immunity and
375 inflammation. In *Nature Reviews Immunology* (Vol. 14, Issue 5, pp. 289–301).
376 <https://doi.org/10.1038/nri3646>

- 377 Pierson, T. C., & Diamond, M. S. (2020). The continued threat of emerging flaviviruses. *Nature*
378 *Microbiology*, 5(6), 796–812. <https://doi.org/10.1038/s41564-020-0714-0>
- 379 Pingen, M., Bryden, S. R., Pondeville, E., Schnettler, E., Kohl, A., Merits, A., Fazakerley, J. K., Graham, G.
380 J., & McKimmie, C. S. (2016). Host Inflammatory Response to Mosquito Bites Enhances the Severity
381 of Arbovirus Infection. *Immunity*, 44(6), 1455–1469. <https://doi.org/10.1016/j.immuni.2016.06.002>
- 382 Pingen, M., Schmid, M. A., Harris, E., & McKimmie, C. S. (2017). Mosquito Biting Modulates Skin
383 Response to Virus Infection. *Trends in Parasitology*, 33(8), 645–657.
384 <https://doi.org/10.1016/j.pt.2017.04.003>
- 385 Prelli Bozzo, C., Nchioua, R., Volcic, M., Koepke, L., Krüger, J., Schütz, D., Heller, S., Stürzel, C. M., Kmiec,
386 D., Conzelmann, C., Müller, J., Zech, F., Braun, E., Groß, R., Wettstein, L., Weil, T., Weiß, J., Diofano,
387 F., Rodríguez Alfonso, A. A., ... Kirchhoff, F. (2021). IFITM proteins promote SARS-CoV-2 infection
388 and are targets for virus inhibition in vitro. *Nature Communications*, 12(1), 1–13.
389 <https://doi.org/10.1038/s41467-021-24817-y>
- 390 Rossi, S. L., Nasar, F., Cardoso, J., Mayer, S. v., Tesh, R. B., Hanley, K. A., Weaver, S. C., & Vasilakis, N.
391 (2012). Genetic and phenotypic characterization of sylvatic dengue virus type 4 strains. *Virology*,
392 423(1), 58–67. <https://doi.org/10.1016/j.virol.2011.11.018>
- 393 Savidis, G., Perreira, J. M., Portmann, J. M., Meraner, P., Guo, Z., Green, S., & Brass, A. L. (2016). The
394 IFITMs Inhibit Zika Virus Replication. *Cell Reports*, 15(11), 2323–2330.
395 <https://doi.org/10.1016/j.celrep.2016.05.074>
- 396 Sourisseau, M., Schilte, C., Casartelli, N., Trouillet, C., Guivel-Benhassine, F., Rudnicka, D., Sol-Foulon, N.,
397 Roux, K. le, Prevost, M.-C., Fsihi, H., Frenkiel, M.-P., Blanchet, F., Afonso, P. v., Ceccaldi, P.-E.,
398 Ozden, S., Gessain, A., Schuffenecker, I., Verhasselt, B., Zamborlini, A., ... Schwartz, O. (2007).
399 Characterization of Reemerging Chikungunya Virus. *PLoS Pathogens*, 3(6), e89.
400 <https://doi.org/10.1371/journal.ppat.0030089>
- 401 Styer, L. M., Kent, K. A., Albright, R. G., Bennett, C. J., Kramer, L. D., & Bernard, K. A. (2007). Mosquitoes
402 inoculate high doses of West Nile virus as they probe and feed on live hosts. *PLoS Pathogens*, 3(9),
403 1262–1270. <https://doi.org/10.1371/journal.ppat.0030132>
- 404 Surasombatpattana, P., Hamel, R., Patramool, S., Luplertlop, N., Thomas, F., Desprès, P., Briant, L., Yssel,
405 H., & Missé, D. (2011). Dengue virus replication in infected human keratinocytes leads to activation
406 of antiviral innate immune responses. *Infection, Genetics and Evolution*, 11(7), 1664–1673.
407 <https://doi.org/10.1016/j.meegid.2011.06.009>
- 408 Svenson, E. L., Moser, L. A., Boylan, B. T., Bernard, K. A., Fedorova, N. B., Pickett, B. E., Moreira, F. R.,
409 Myers, L. J., Svenson, E. L., Fedorova, N. B., Pickett, B. E., & Bernard, K. A. (2018). Growth and
410 adaptation of Zika virus in mammalian and mosquito cells. *PLOS Neglected Tropical Diseases*,
411 12(11), e0006880. <https://doi.org/10.1371/journal.pntd.0006880>
- 412 Waggoner, J. J., Rojas, A., Mohamed-Hadley, A., de Guillén, Y. A., & Pinsky, B. A. (2018). Real-time RT-
413 PCR for Mayaro virus detection in plasma and urine. *Journal of Clinical Virology*, 98(12), 1–4.
414 <https://doi.org/10.1016/j.jcv.2017.11.006>

415 Weaver, S. C., Costa, F., Garcia-Blanco, M. A., Ko, A. I., Ribeiro, G. S., Saade, G., Shi, P. Y., & Vasilakis, N.
416 (2016). Zika virus: History, emergence, biology, and prospects for control. *Antiviral Research*, *130*,
417 69–80. <https://doi.org/10.1016/j.antiviral.2016.03.010>

418 Wichit, S., Diop, F., Hamel, R., Talignani, L., Ferraris, P., Cornelie, S., Liegeois, F., Thomas, F., Yssel, H., &
419 Missé, D. (2017). *Aedes Aegypti* saliva enhances chikungunya virus replication in human skin
420 fibroblasts via inhibition of the type I interferon signaling pathway. *Infection, Genetics and*
421 *Evolution*, *55*(June), 68–70. <https://doi.org/10.1016/j.meegid.2017.08.032>

422 Zhao, X., Li, J., Winkler, C. A., An, P., & Guo, J. T. (2019). IFITM genes, variants, and their roles in the
423 control and pathogenesis of viral infections. *Frontiers in Microbiology*, *10*(JAN), 1–12.
424 <https://doi.org/10.3389/fmicb.2018.03228>

425

426 **Acknowledgment:** The authors would like to acknowledge the anonymous donors for providing skin
427 tissue used in this study.

428 **Funding:** The study described in this manuscript was funded by Departmental Start-up funds and SUNY
429 Empire Innovation Professorship funds to ST

430 **Conflict of interest:** The authors state no conflict of interests.

431

432 **Author contributions:**

433 Conception: ST and ATE

434 Experimental design: ATE, JF, MG, ST

435 Resources: ST, PU, JM

436 Acquisition of data and analysis: ATE, PU

437 Interpretation of data: ATE and ST

438 Supervision: ST

439 Writing-Original Draft preparation: ATE

440 Writing-Review and Editing: ATE, JF, MG, PU, ST

441 Funding acquisition: ST

442

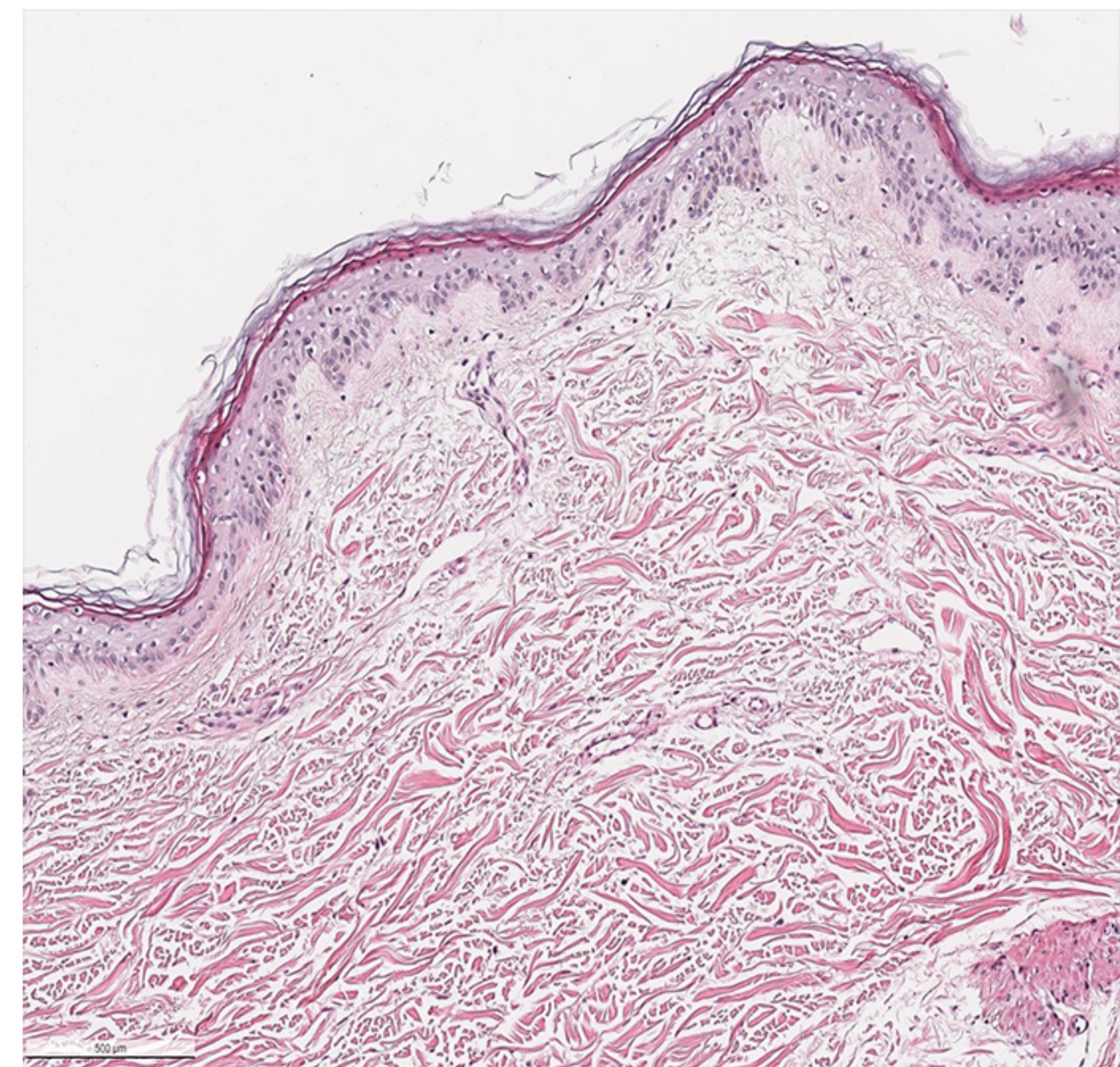
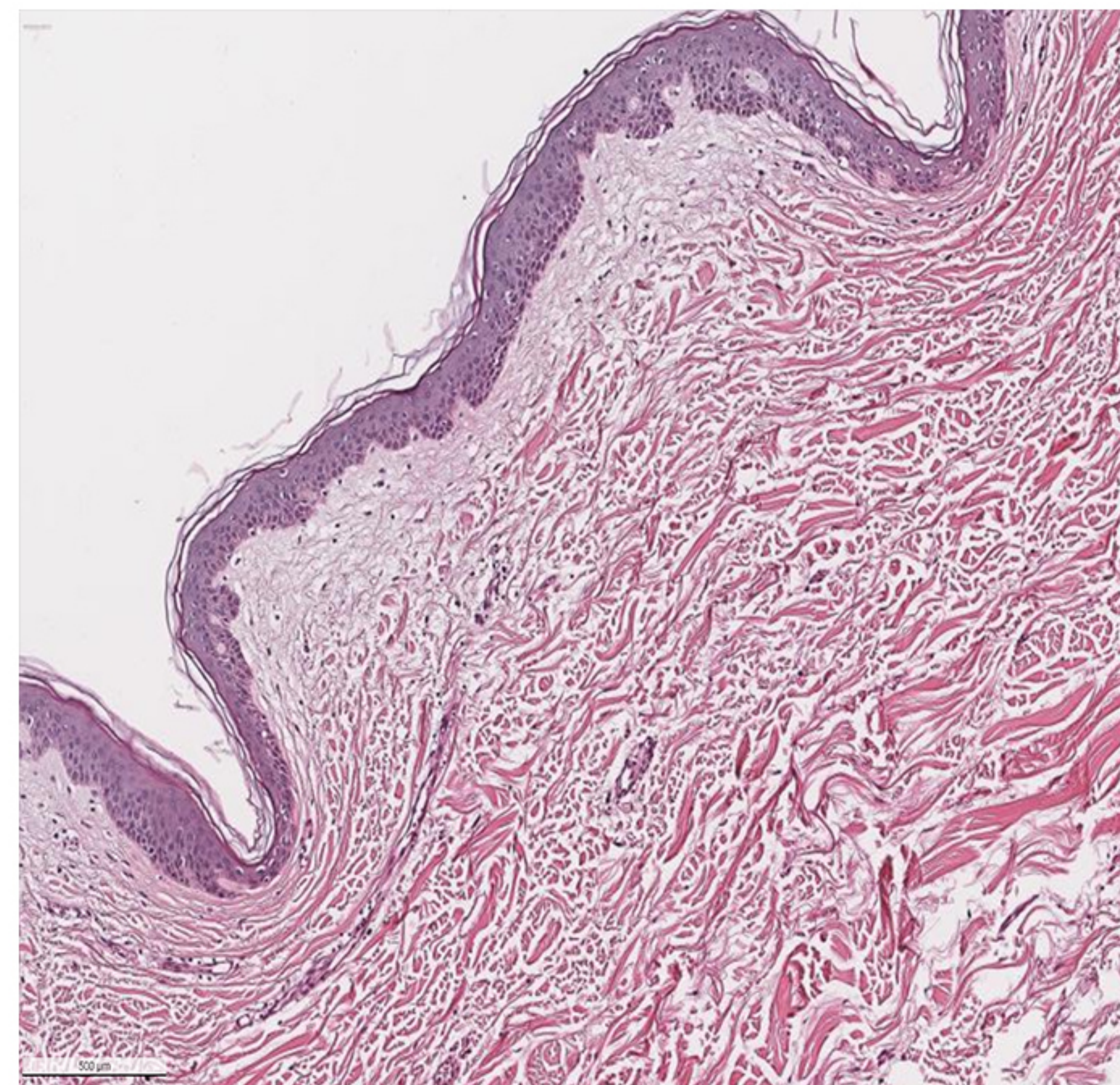
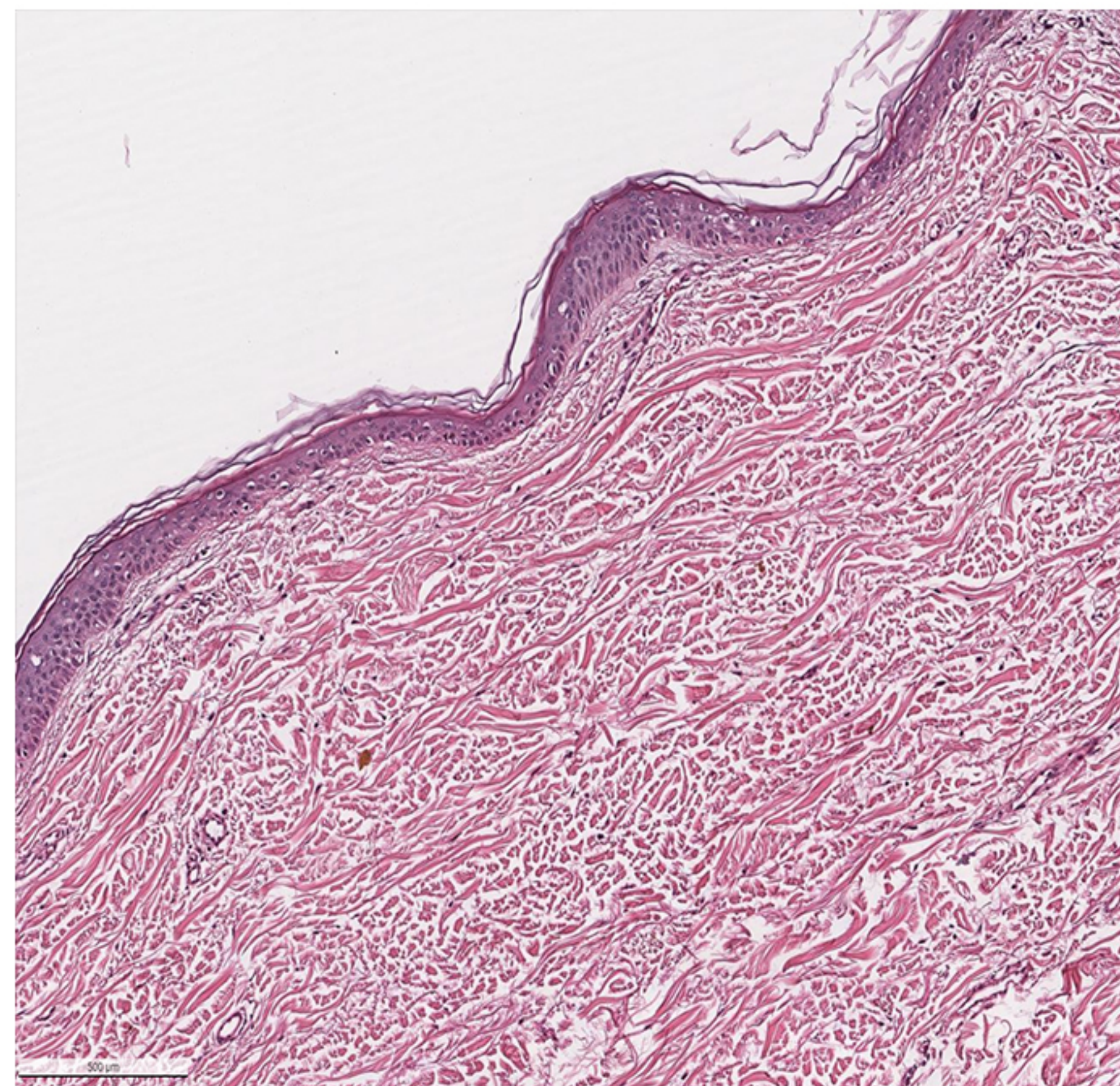
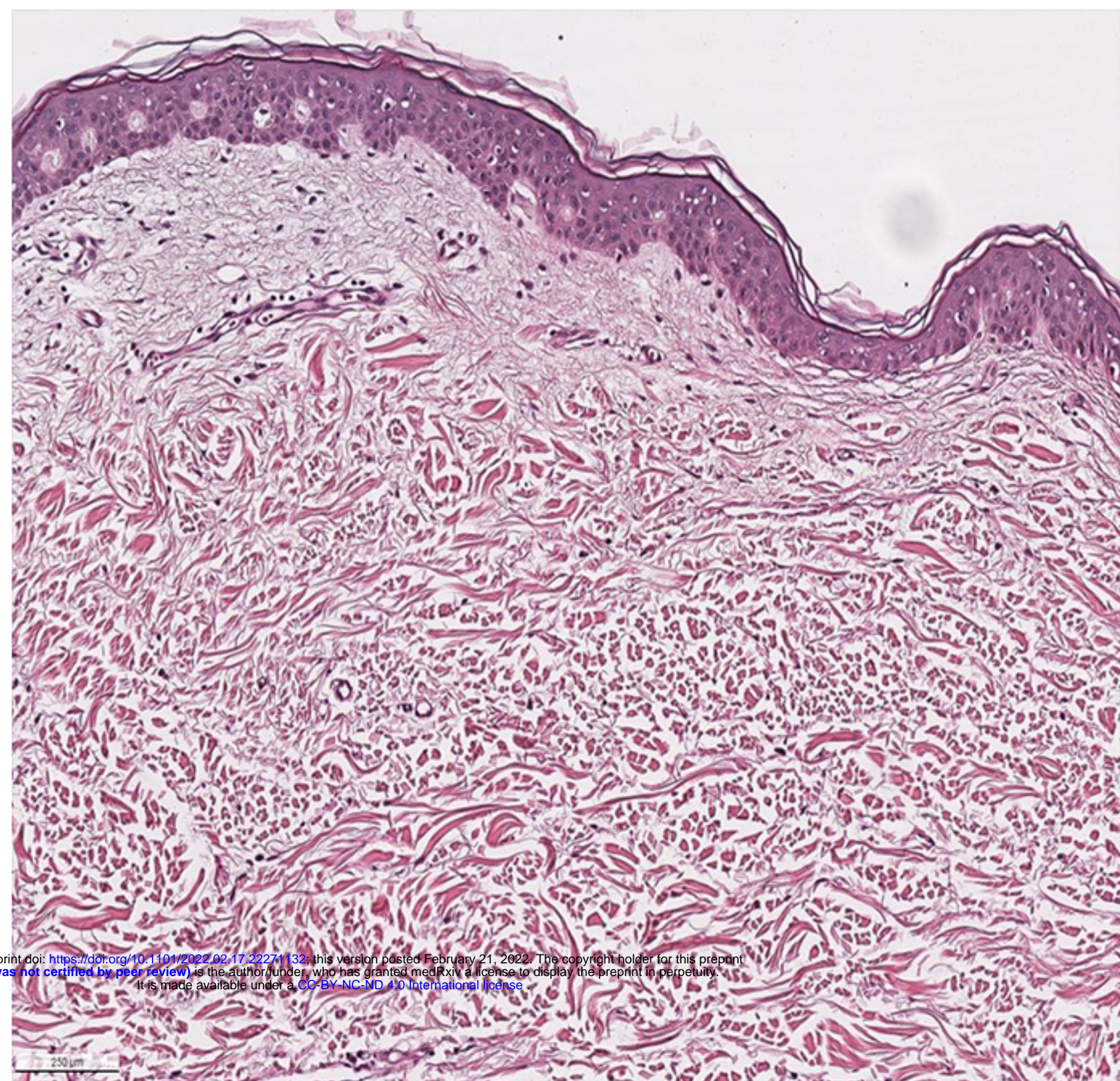
Day 1

Day 2

Day 3

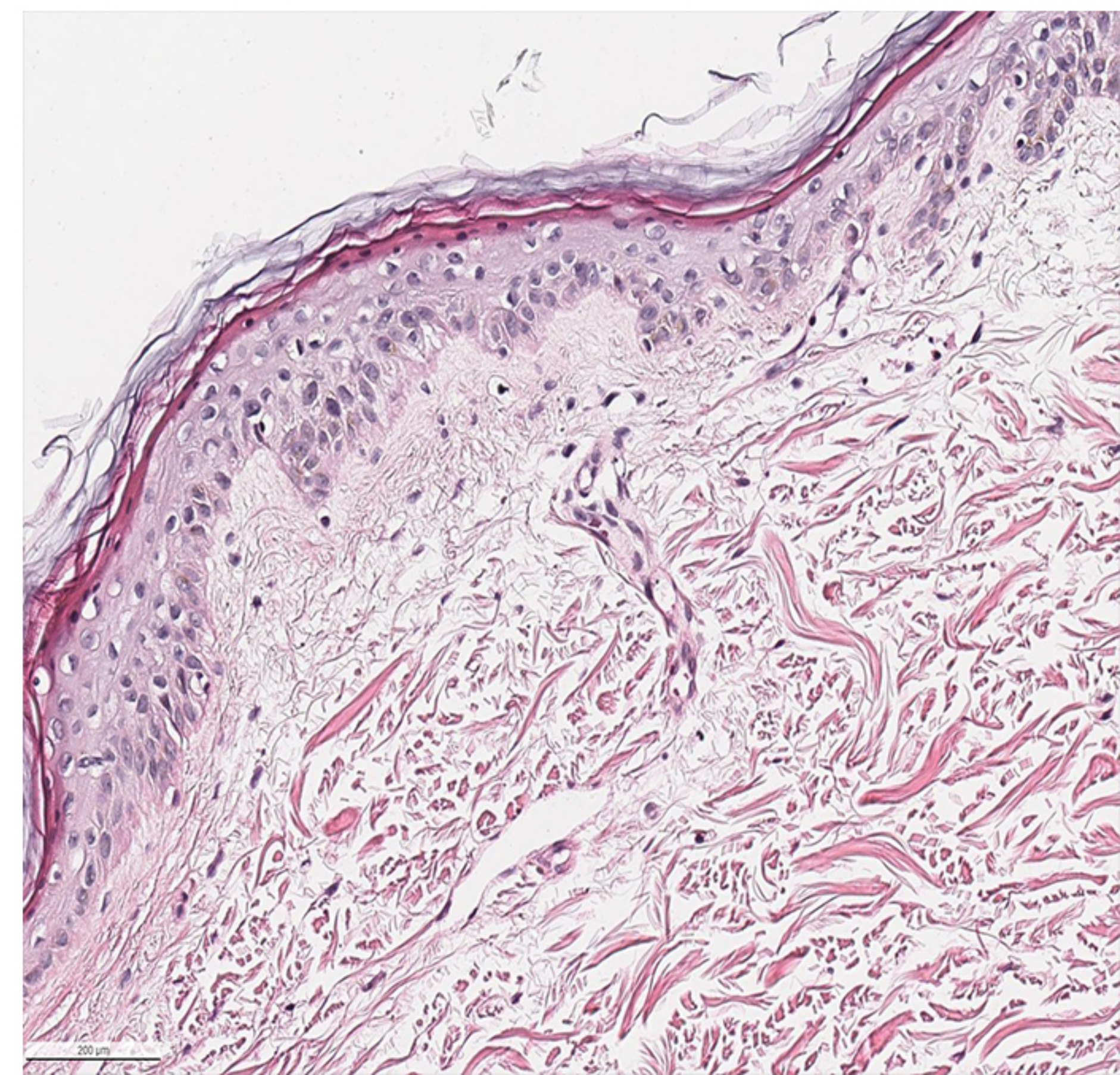
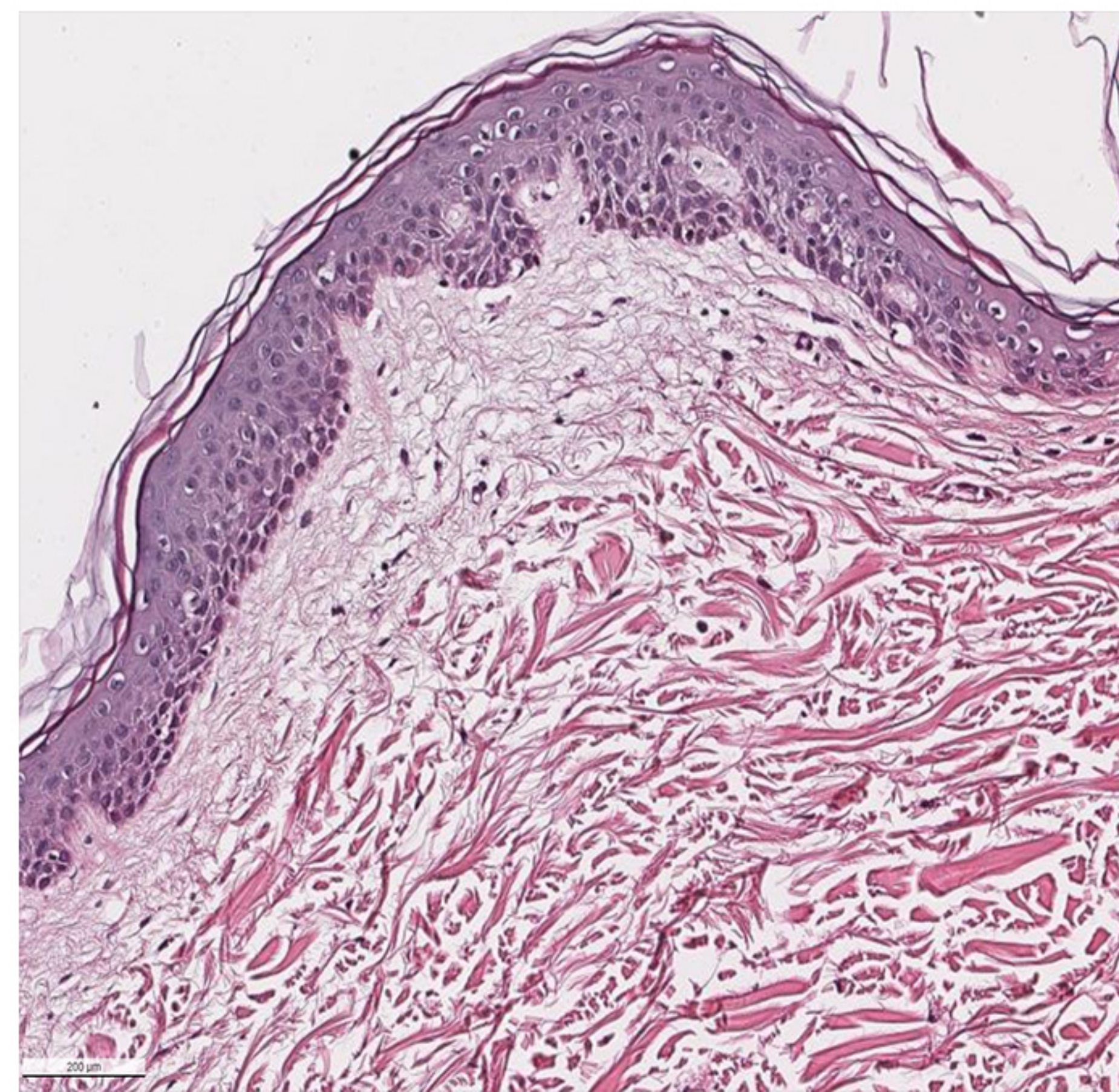
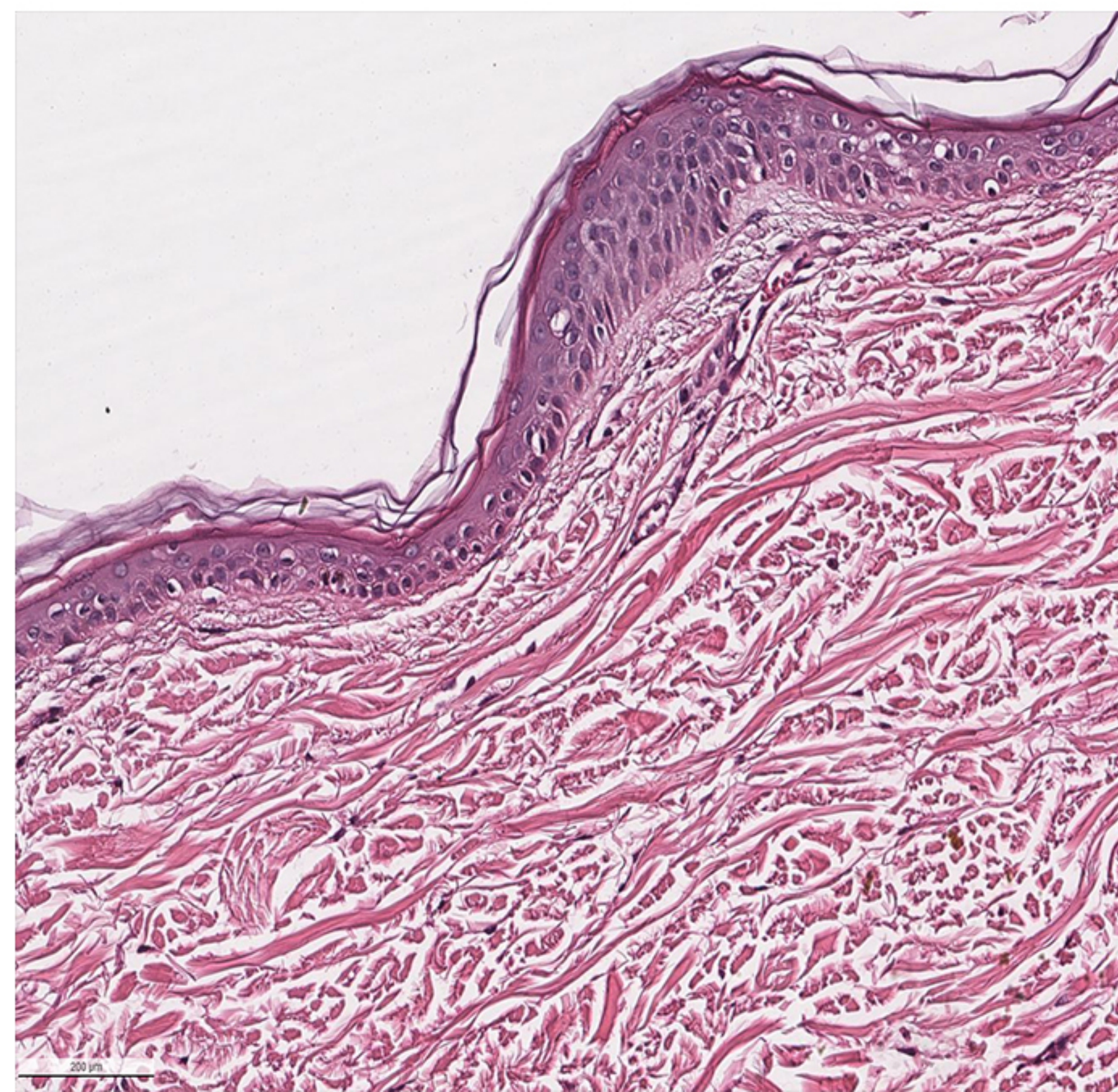
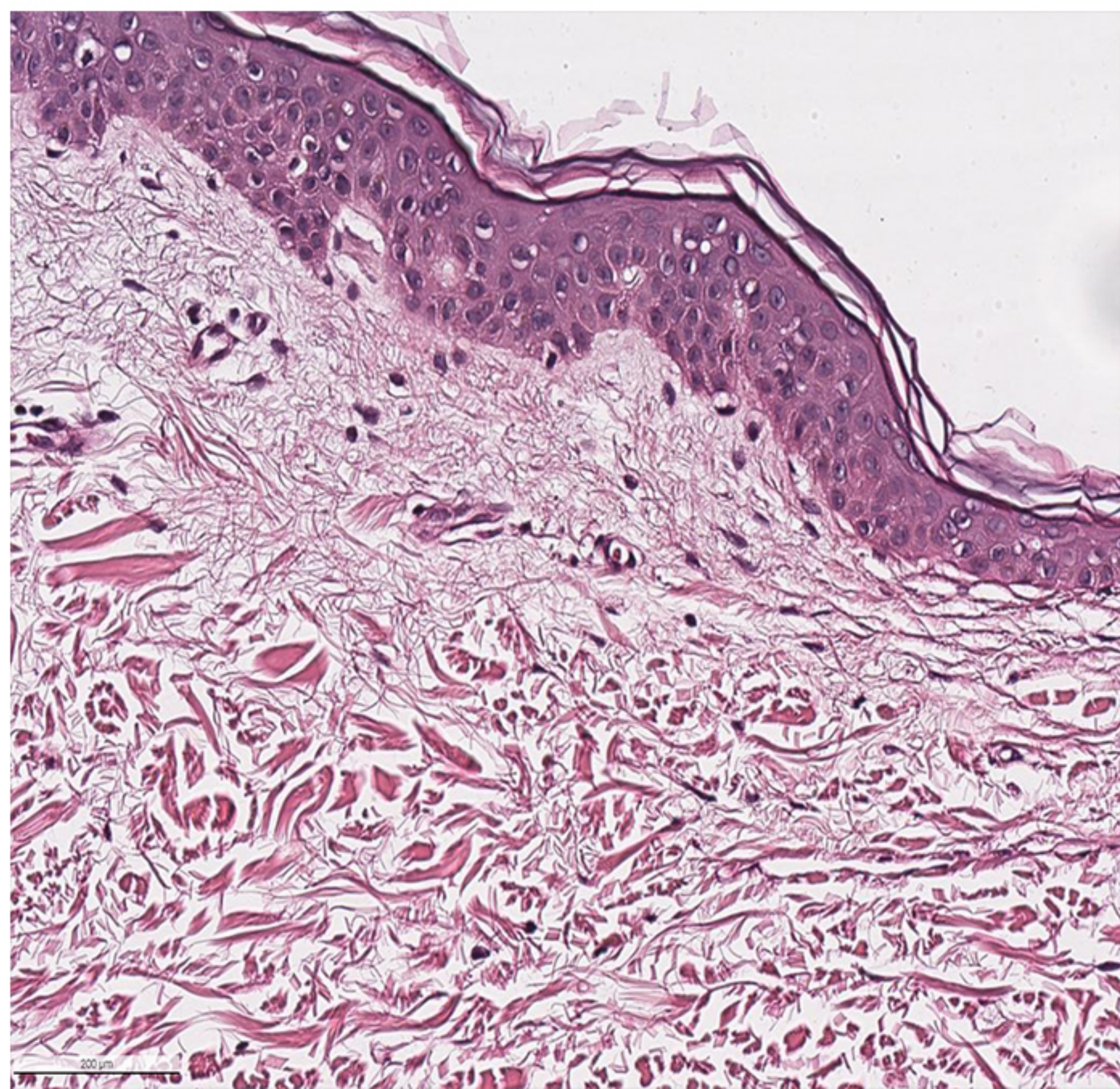
Day 4

10x

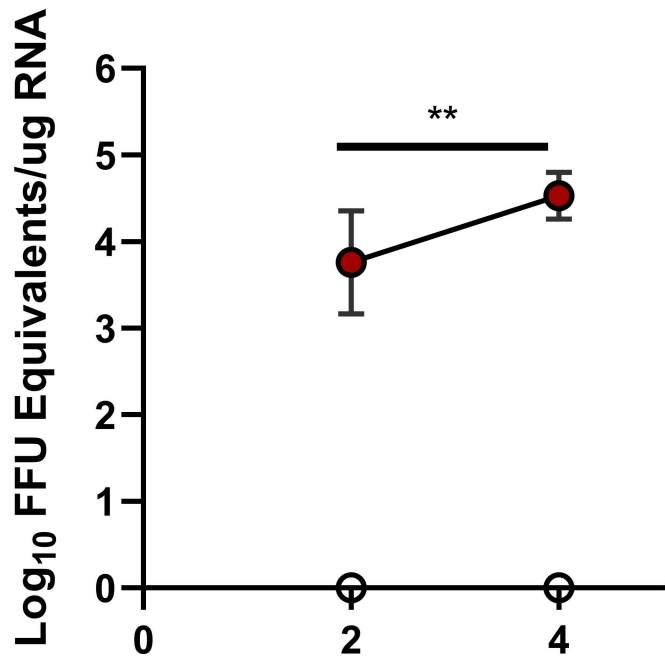


medRxiv preprint doi: <https://doi.org/10.1101/2021.02.21.21011101>; this version posted February 21, 2021. The copyright holder for this preprint (which was not certified by peer review) is the author/funder, who has granted medRxiv a license to display the preprint in perpetuity. It is made available under aCC-BY-NC-ND 4.0 International license.

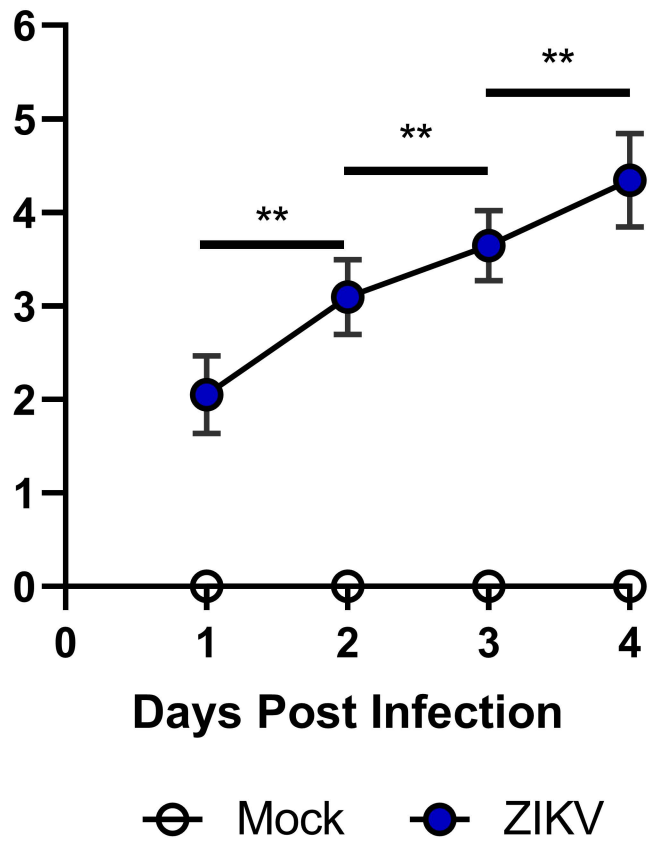
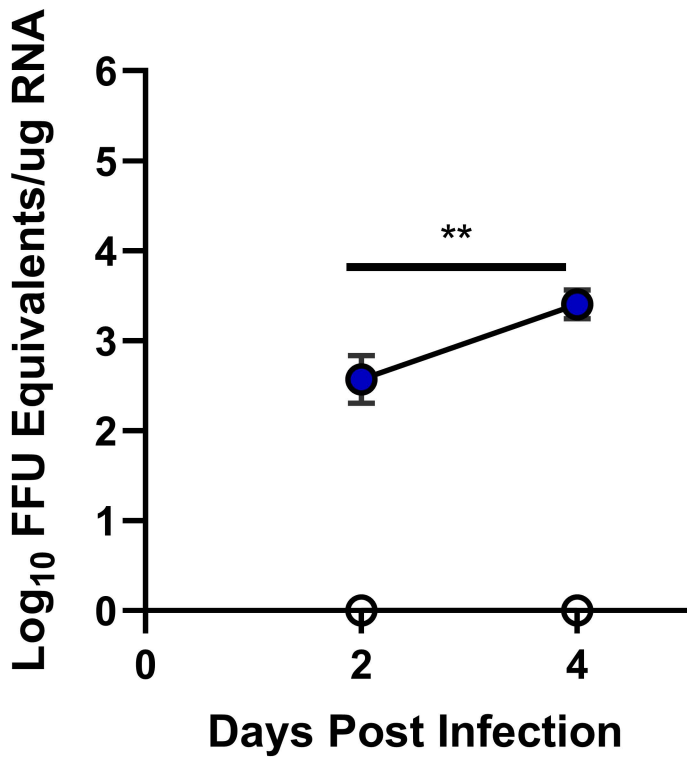
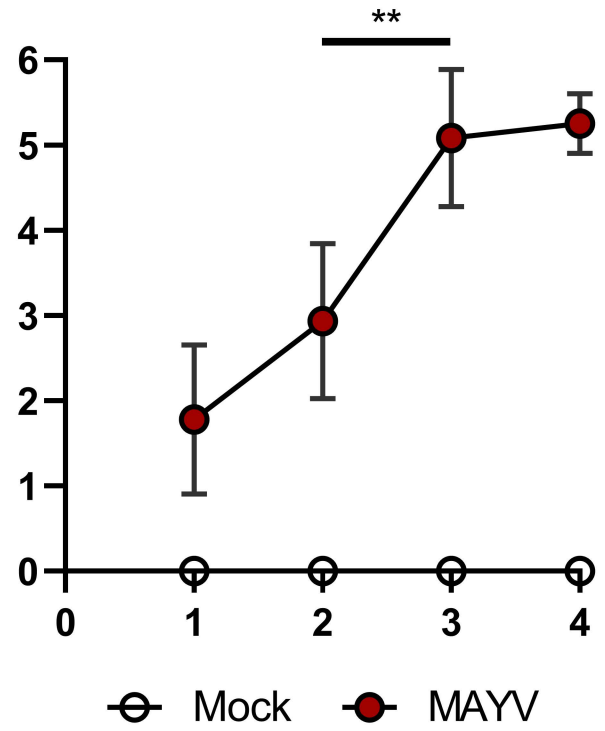
20x



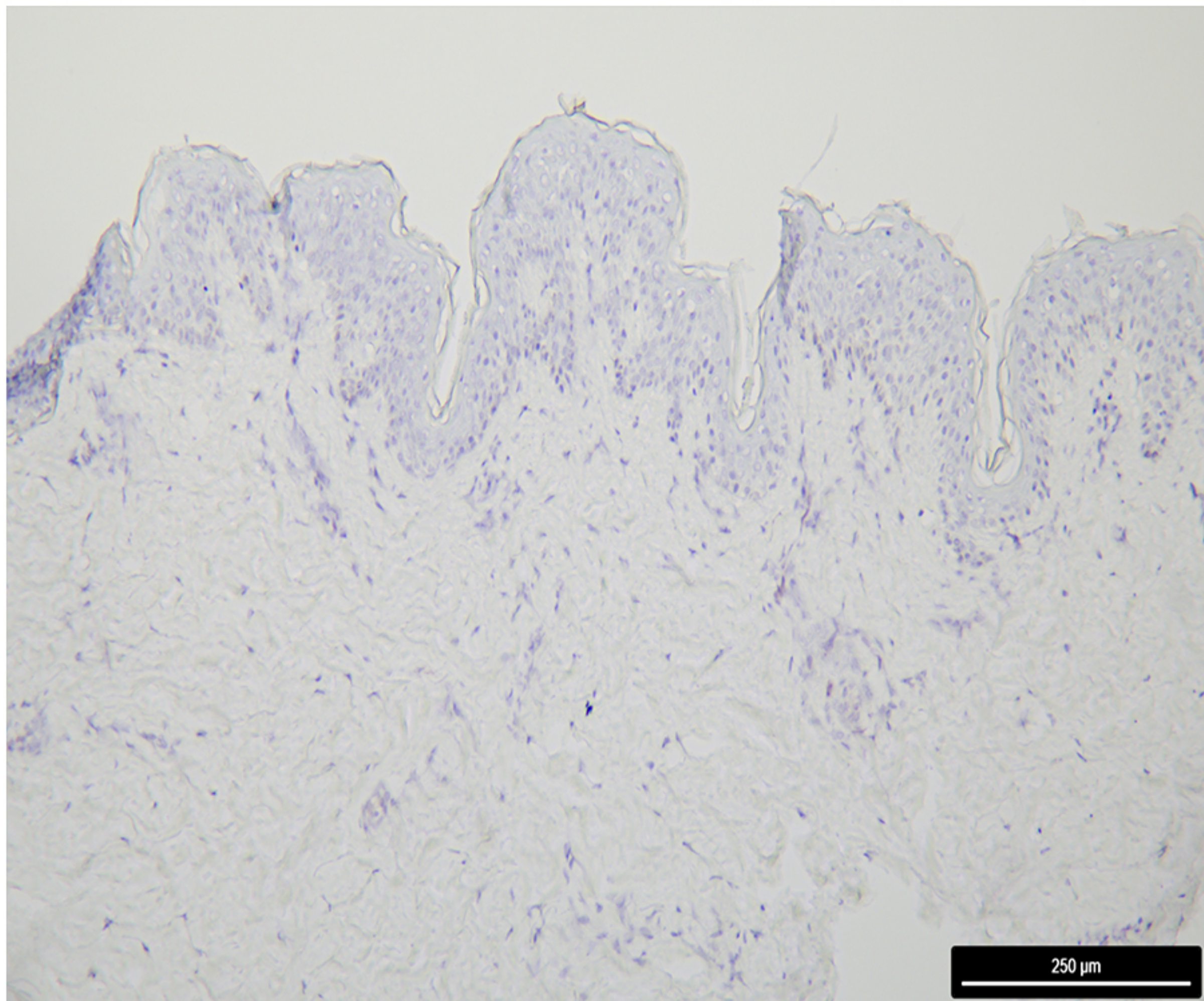
Skin



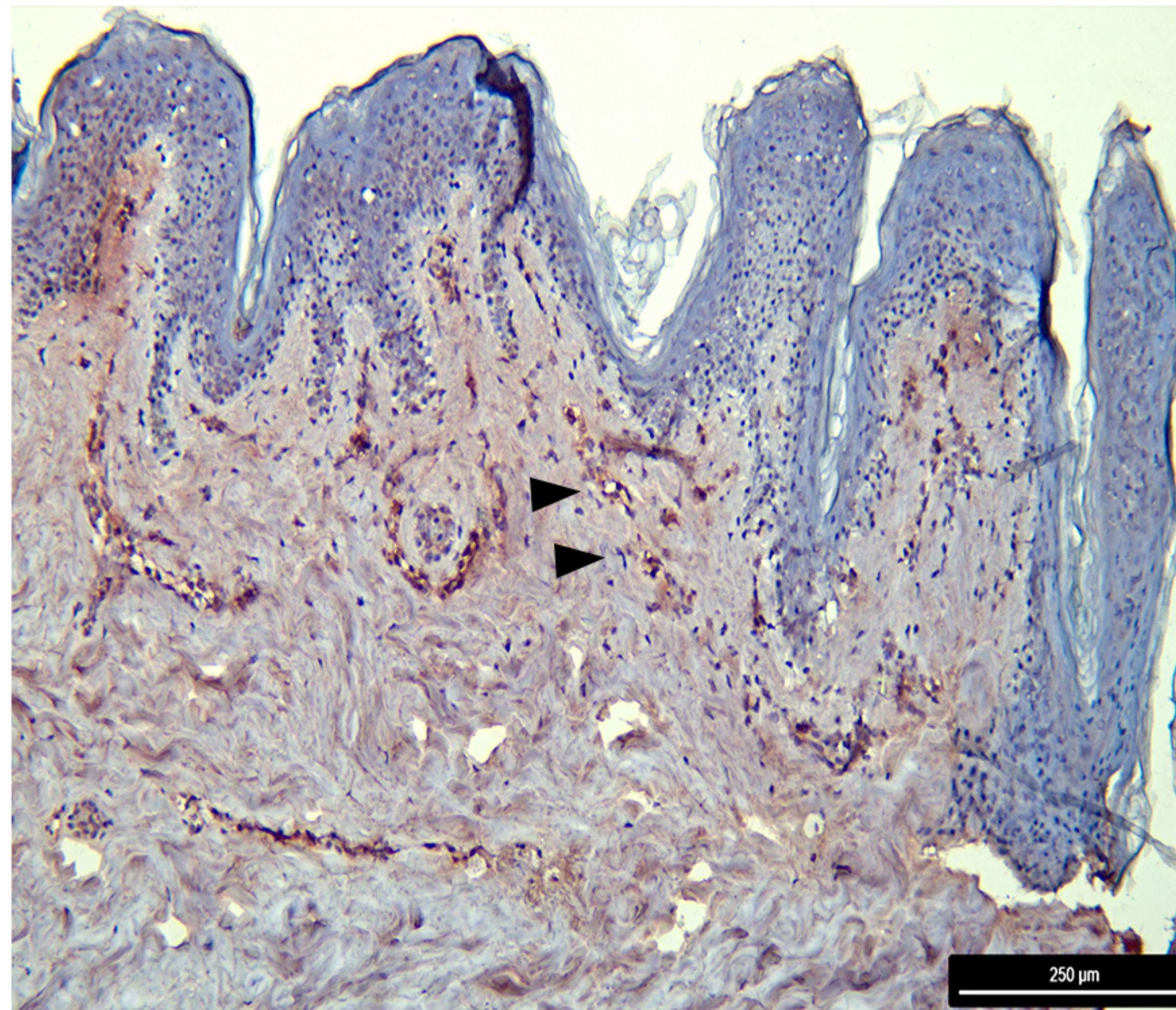
Culture Media



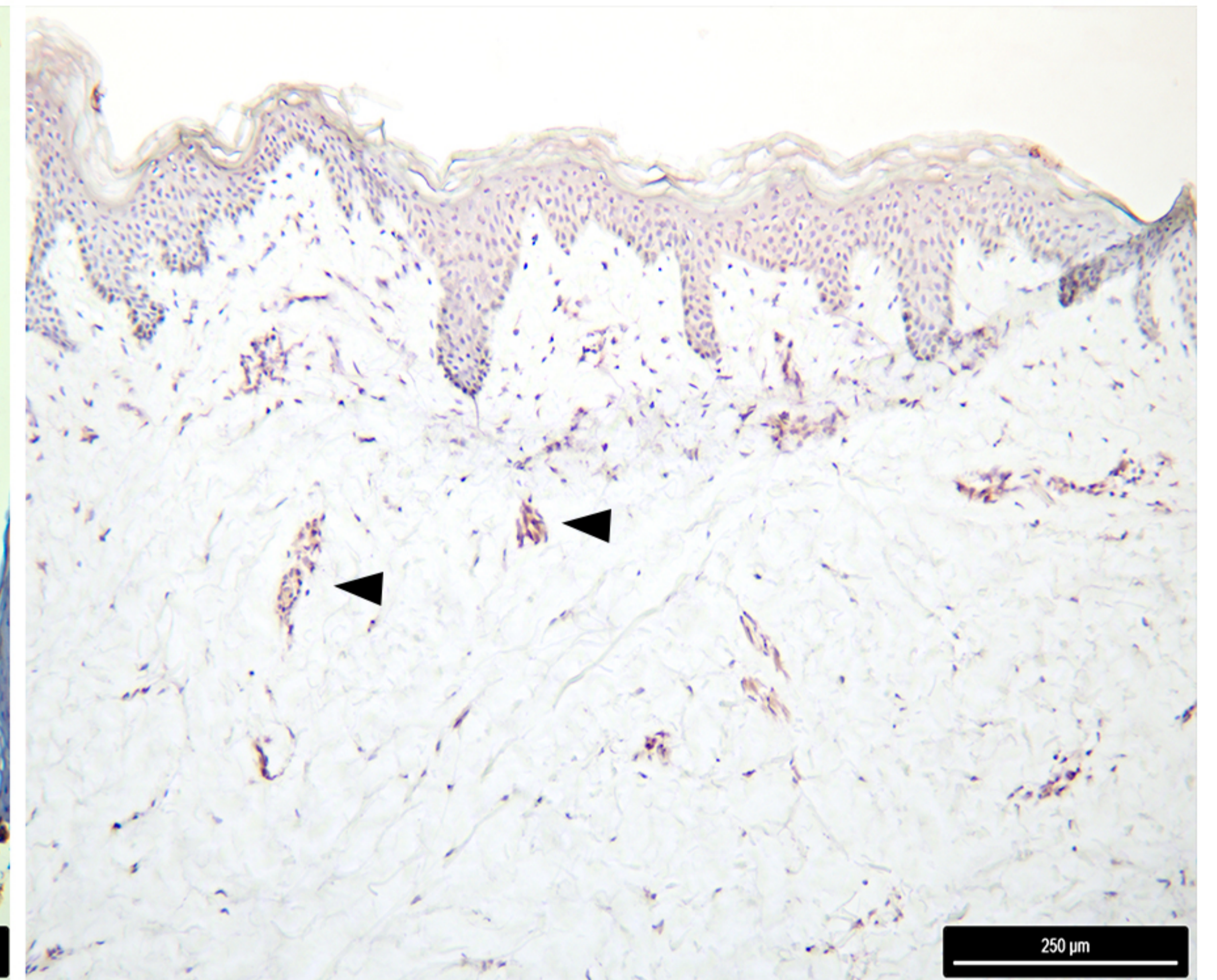
Mock Infected



MAYV Infected



ZIKV Infected



medRxiv preprint doi: <https://doi.org/10.1101/2022.02.17.22271132>; this version posted February 21, 2022. The copyright holder for this preprint (which was not certified by peer review) is the author/funder, who has granted medRxiv a license to display the preprint in perpetuity. It is made available under a CC-BY-NC-ND 4.0 International license.

